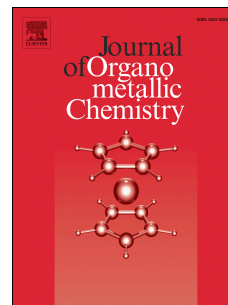


Accepted Manuscript

Facile synthesis of magnetic recyclable palladium-gold alloy nanoclusters catalysts PdAu_r/Fe₃O₄@LDH and its catalytic applications in Heck reaction

Jin Li, Yajuan Wang, Shunwang Jiang, Hui Zhang



PII: S0022-328X(18)30687-9

DOI: [10.1016/j.jorganchem.2018.10.007](https://doi.org/10.1016/j.jorganchem.2018.10.007)

Reference: JOM 20592

To appear in: *Journal of Organometallic Chemistry*

Received Date: 6 August 2018

Revised Date: 28 September 2018

Accepted Date: 14 October 2018

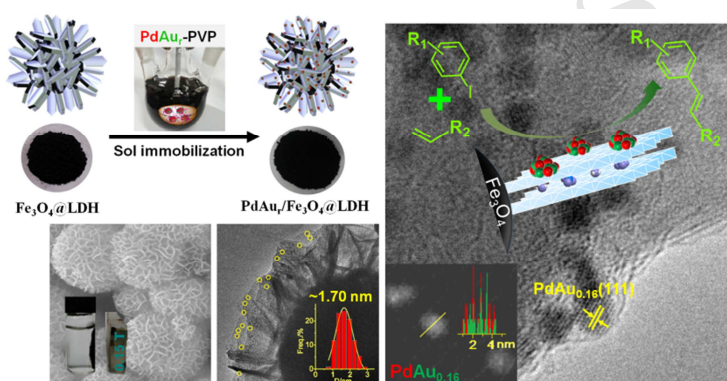
Please cite this article as: J. Li, Y. Wang, S. Jiang, H. Zhang, Facile synthesis of magnetic recyclable palladium-gold alloy nanoclusters catalysts PdAu_r/Fe₃O₄@LDH and its catalytic applications in Heck reaction, *Journal of Organometallic Chemistry* (2018), doi: <https://doi.org/10.1016/j.jorganchem.2018.10.007>.

This is a PDF file of an unedited manuscript that has been accepted for publication. As a service to our customers we are providing this early version of the manuscript. The manuscript will undergo copyediting, typesetting, and review of the resulting proof before it is published in its final form. Please note that during the production process errors may be discovered which could affect the content, and all legal disclaimers that apply to the journal pertain.

Facile synthesis of magnetic recyclable palladium-gold alloy nanoclusters catalysts PdAu₁/Fe₃O₄@LDH and its catalytic applications in Heck reaction

Jin Li[‡], Yajuan Wang[‡], Shunwang Jiang and Hui Zhang^{*}

Graphical Abstract





Facile synthesis of magnetic recyclable palladium-gold alloy nanoclusters catalysts PdAu_r/Fe₃O₄@LDH and its catalytic applications in Heck reaction

Jin Li[‡], Yajuan Wang[‡], Shunwang Jiang and Hui Zhang^{*}

State Key Laboratory of Chemical Resource Engineering, Beijing University of Chemical Technology, P.O. Box 98, Beijing, 100029; P. R. China

ARTICLE INFO

Article history:

Received
Received in revised form
Accepted
Available online

Keywords:

PdAu alloy nanoclusters
core@shell structure
magnetism
Heck reaction

ABSTRACT

A series of novel magnetic recyclable Pd-Au nanoclusters (NCs) catalysts x-PdAu_r/Fe₃O₄@LDH (x: Pd loading in wt%, r: Au/Pd molar ratio, LDH: layered double hydroxide, here refers the typical MgAl-LDH) were synthesized by a facile polyol reduction followed sol immobilization of PdAu_r-PVP on core@shell support Fe₃O₄@LDH. Systematic characterizations reveal that the obtained catalysts possess the honeycomb-like core@shell, and the ultrafine PdAu alloy nanoclusters with the size in 1.70–2.55 nm highly dispersed on the LDH nanoplates shell. The obtained catalysts 1.0-PdAu_r/Fe₃O₄@LDH (r: 0.11, 0.16 and 0.48) show higher Heck activity of iodobenzene with styrene than monometallic ones, especially 1.0-PdAu_{0.16}/Fe₃O₄@LDH displays the highest Heck activity under the optimal condition. Moreover, the catalysts can be applied for the Heck reaction of a variety of aryl halides with alkenes, and can be conveniently separated by an external magnet and reused ten runs without significant loss of activity.

2018 Elsevier Ltd. All rights reserved.

1. Introduction

Palladium-catalyzed Heck coupling reaction are important means for the construction of C-C bands between aryl halides and alkenes [1-3], and is applied widely in the synthesis of natural products [4], pharmaceuticals [5] and fine chemicals [6]. Heterogeneous Pd catalysts [7-11] applied in the Heck reaction is favored over conventional homogeneous Pd catalysts [12-14] because of the low-cost, easy separation for reusability, and environment-friendliness of the former, thus becoming a preferred alternative. In order to develop highly active Pd-based catalysts, alloying Pd with a second metal has proved to be a promising research strategy [15-20] owing to their unique physical and chemical properties which are different significantly from their monometallic counterparts. Among the Pd-based alloy catalysts fabricated so far, PdAu alloy catalysts are especially fascinating due to the obviously enhanced catalytic performance in methane oxidation [16], phenyl isocyanide oxidation [17] and C-C coupling reactions [18-20]. Chen *et al.* [19] prepared AuPd alloy nanocrystals enveloped in SiO₂ nanorattles (AuPd@SiO₂) via one-pot hydrothermal method, and the obtained Au₃Pd₁@SiO₂ (~8.1 nm) catalyst showed a higher Suzuki reaction activity (bromobenzene conversion: 99.8% and biphenyl selectivity: 99.3%, 30 min) than Pd@SiO₂. Khashab *et al.* [20] reported oleylamine-Au₄₂Pd₅₈ alloy NPs (10-15 nm) catalyst by high temperature chemical reduction of AuCl₃ and PdCl₂ and Au@Pd core-shell nanobranches one by oleylamine-Au NPs (33 nm)-mediated method with CTAB as phase transfer agent

followed PdCl₂ reduction by ascorbic acid, and the latter showed higher yield of stilbene (90%, 3 h) in the Heck reaction of iodobenzene with styrene than the former (80%, 3 h) due to Au@Pd core-shell nanobranches exposing more active sites. However, the study on PdAu alloy catalysts for the Heck reaction is rarely published in previous reports except one [20], far from the tiny PdAu alloy nanoclusters catalyst. Moreover, the separation of previously reported PdAu alloy catalysts suffers from time- and power-consuming. Therefore, development of highly active and easily recyclable PdAu bimetallic alloy nanoclusters catalysts for the Heck reaction is highly desired.

Recently, magnetic core@shell nanocomposite with multi-functional combination, as an extraordinary candidate to traditional supports for preparing high performance catalysts, has drawn increasing attention [21-23] because of its unique advantages of both core and shell evolving (1) magnetic characteristic of core with efficient separation for reusability, and (2) well-defined dispersion of active metal sites, or/and intrinsic acid/basic sites for promoting catalytic activity. Xu *et al.* [21] prepared SiO₂-coated iron oxide (Fe₃O₄/SiO₂) hybrid modified by multicarboxylic hyperbranched polyglycerol (HPG) followed directly growth of Pd NPs (4.0 ± 0.4 nm) from Pd(NO₃)₂ reduced by NaBH₄ giving Fe₃O₄/SiO₂/HPG-Pd catalyst, which showed high activity for the Heck reaction of iodobenzene (PhI) with styrene at 140 °C using base additive NaOAc in DMF (stilbene yield: 93%, 6 h) and slight loss of activity in the 4th run on magnetic separation. However, though these magnetic core@shell Pd-based catalysts show excellent catalytic property, the preparation and surface modification of the magnetic core@shell support suffers from long operation periods and tedious synthetic procedures, which greatly limits the practical application of such core@shell materials. The layered double hydroxide (LDH), as a typical layered material, has been widely

[‡]These authors contributed equally to this work.

^{*}Corresponding author. Tel: +8610-6442 5872; Fax: +8610-6442 5385. E-mail addresses: huizhang67@gst21.com.

applied in catalysis owing to its adjustable surface acidity-basicity, high surface area and uniquely positively-charged 2-dimensional hydroxide nanolayers [24]. Combination of magnetic iron oxide with LDH, which contains the easy separation of magnetic material and the advantages of LDH, is a promising class of magnetic composites. Zhang *et al.* [25,26] reported a novel core@shell hybrid $\text{Fe}_3\text{O}_4@\text{MgAl-LDH}$ via a one-step coprecipitation as superparamagnetic support loading nanogold for highly efficient oxidation of 1-phenylethanol without base addition, and it showed good recyclability upon magnetic separation. Additionally, it is reported that the basic surface of the LDH can greatly facilitate the oxidative addition step in the Heck reaction [11]. Clearly, assembly of magnetic recyclable LDH supported Pd-Au bimetallic nanoclusters catalysts for the Heck reaction is highly desired.

Herein, a series of novel hierarchical magnetic core@shell catalysts $x\text{-PdAu}_r/\text{Fe}_3\text{O}_4@\text{LDH}$ (x : Pd loading in wt%, r : Au/Pd molar ratio) were fabricated by a facile polyol reduction-immobilization method and systematically characterized. The effect of Au/Pd ratios and Pd loadings on the size and size distribution, electron density and surface compositions of PdAu nanoclusters on the catalysts with unique honeycomb-like core@shell structure, thus on the Heck reactivity was deeply studied. The reaction rate constant and apparent activation energy of the Heck reaction over the present catalysts are determined. Moreover, the substrate adaptability and recyclability of the catalyst was tested.

2. Experimental section

2.1 Materials

All chemicals were of analytical grade and used as received without further purification. Ethylene glycol (EG), K_2CO_3 , KCl and N, N-dimethylformamide (DMF) were supplied from Beijing Chemical Works, and poly (N-vinyl-2-pyrrolidone) (PVP, MW = 58000) from XiLong Chemical Corporation. PdCl_2 , styrene and bromobenzene were purchased from Tianjin Fuchen Chemical Reagents Factory, and $\text{HAuCl}_4\cdot 4\text{H}_2\text{O}$ from Sinopharm Chemical Reagent Co., Ltd.. Methyl acrylate, ethyl acrylate, iodobenzene and other aryl halides were purchased from Aladdin. The deionized water with a resistivity $> 18.25 \text{ M}\Omega \text{ cm}$ (25°C) was employed in the whole work.

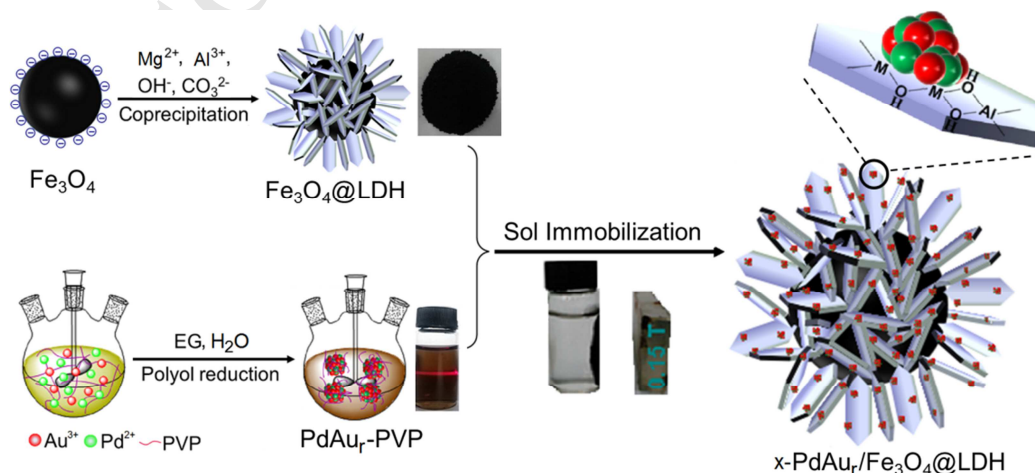
2.2 Synthesis of magnetic support

Submicrospheres Fe_3O_4 (~526 nm) were prepared via a surfactant-free solvothermal method in our previous work [27]. Next, the black Fe_3O_4 powder (1.0 g) were ultrasonically dispersed in deionized water (100 mL) to give an uniform

suspension. An alkaline aq. solution (100 mL) of NaOH (0.02 mol) and Na_2CO_3 (0.006 mol) was added dropwise into the above suspension until pH ~10 and kept for 5 min. Then, another aq. solution (100 mL) of $\text{Mg}(\text{NO}_3)_2\cdot 6\text{H}_2\text{O}$ (0.009 mol) and $\text{Al}(\text{NO}_3)_3\cdot 9\text{H}_2\text{O}$ (0.003 mol) was added dropwise into the above suspension under vigorously stirring with constant pH of 10 kept by simultaneously adding above alkaline solution. The black slurry was magnetically separated by a NdFeB magnet (0.15 T), washed by water until pH ~7, and dried at 60°C overnight giving the support $\text{Fe}_3\text{O}_4@\text{MgAl-LDH}$ (denoted as $\text{Fe}_3\text{O}_4@\text{LDH}$). The reference support MgAl-LDH (denoted as LDH) was prepared according to our previous work [28].

2.3 Synthesis of magnetic PdAu alloy nanoclusters catalysts

The synthesis of PdAu_r-PVP alloy nanoclusters (NCs) with varied Au/Pd molar ratios were realized via a polyol reduction method according to the previous report [29]. Typically, 0.97 g PVP was dissolved into an aq. solution (150 mL) containing K_2PdCl_4 (0.141 mmol PdCl_2 and 0.282 mmol KCl) and $\text{HAuCl}_4\cdot 4\text{H}_2\text{O}$ (0.0254 mmol) with Au/Pd ratio of 0.18 and PVP/(Pd+Au) ratio of 0.1 under vigorous stirring followed adding 50 mL EG at room temperature. Then the resultant was refluxed at 140°C for 2 h forming a dark brown colloidal dispersion. After cooling to room temperature, the support $\text{Fe}_3\text{O}_4@\text{LDH}$ (1 g, the amount of support was fixed on a designed Pd loading of 1.5 wt%) was added to the above colloidal dispersion under vigorous stirring and kept for 1 h to immobilize the PdAu_r-PVP colloid on the surface of support. The resultant was magnetically separated by a magnet, washed and dried at 60°C for 24 h to yield a black powder denoted as 1.0-PdAu_{0.16}/ $\text{Fe}_3\text{O}_4@\text{LDH}$ (both Au/Pd ratio 0.16 and Pd loading 1.0 wt% upon ICP). The catalysts with varied Pd loadings were obtained by adjusting amount of the magnetic support resulting in products $x\text{-PdAu}_{0.16}/\text{Fe}_3\text{O}_4@\text{LDH}$ with $x = 0.5, 0.1$ and 0.05 (by ICP), respectively. Then, adjusting the amount of $\text{HAuCl}_4\cdot 4\text{H}_2\text{O}$ to 0, 0.0155 and 0.0761 mmol in 150 mL aq. solution of K_2PdCl_4 and $\text{HAuCl}_4\cdot 4\text{H}_2\text{O}$ on Au/Pd = 0, 0.11 and 0.54 and the amount of PVP to 0.82, 0.91 and 1.26 g on PVP/(Pd+Au) = 0.1, respectively, and keep other conditions constant, giving the monometallic catalyst Pd/ $\text{Fe}_3\text{O}_4@\text{LDH}$ and bimetallic catalysts 1.0-PdAu_r/ $\text{Fe}_3\text{O}_4@\text{LDH}$ ($r = 0.11, 0.48$ on ICP). The monometallic catalyst Au/ $\text{Fe}_3\text{O}_4@\text{LDH}$ -1 was prepared by Au nanoclusters precursor method according to our previous work (details in Electronic Supplementary Information (ESI)) [26]. Scheme 1 depicts the design schematic of the magnetic PdAu alloy nanoclusters catalysts.



Scheme 1. The design schematic of the magnetic PdAu alloy nanoclusters catalysts.

In situ diffuse reflection infrared Fourier transform spectroscopy (DRIFTS) was carried out on a Bruker Vertex 70 instrument containing a controlled environment chamber equipped with CaF₂ windows to study the surface structure and composition of metallic NCs on the catalyst. The DRIFTS spectra were recorded by using wafers in the form of self-supporting pellets of the catalysts powder mounted in a homemade ceramic cell. The catalyst was pretreated in Ar flow (50 mL/min) at 25 °C for 0.5 h. The sample was scanned to get a background record. Then catalyst was exposed to a CO flow (50 mL/min) for 1 h, subsequently the cell was purged with Ar for 1 h. Finally measurement was conducted in Ar atmosphere at 4cm⁻¹ resolution by averaging 64 scans. Hydrogen temperature-programmed reduction (TPR) was realized on a Micrometric ChemiSorb 2750 chemisorption instrument equipped with a thermal conductivity detector. The sample (30 mg) was loaded into the bottom of a quartz reactor and heated from 25 °C to 150 °C with a heating rate of 5 °C/min in Ar flow (50 mL/min) and kept for 1 h, then cooled to 25 °C, followed by keeping a stream of 10% H₂ in Ar (50 cm³ min⁻¹) with a heating rate of 5 °C/min from 25 °C to 300 °C. TGA-MS thermograms for surface transient organometallic intermediate (named as STOI, preparation details in ESI) of the Heck reaction were recorded on a PerkinElmer Diamond TG/DTA/DSC ThermoStar™ instrument to explore the Heck reaction mechanism. In the experiment, the sample (6.4 mg) was heated from 20 °C to 900 °C (10 °C/min) in a N₂ flow. ¹H and ¹³C NMR spectra of the coupling products (dissolved in CDCl₃) were obtained on an AV600 NMR spectrometer (Germany) operating at 600.13 MHz relative to tetramethylsilane (TMS, 0.00 ppm). The other characterization techniques and instruments including powder X-ray diffraction (XRD), FT-IR, inductively coupled plasma atomic emission spectroscopy (ICP-AES), SEM, (HR)TEM, N₂ adsorption-desorption isotherm, high-angle annular dark-field scanning transmission electron microscopy (HAADF-STEM), vibrating sample magnetometer (VSM) and X-ray photoelectron spectrometer (XPS) were identical to our previous reports [26,28].

2.5 Catalytic activity test

The Heck reaction was carried out in a 25-milliliter three-necked flask attached a reflux condenser under magnetic stirring. Aryl halide (1.0 mmol), alkene (1.5 mmol), K₂CO₃ (3 mmol), catalyst (0.3 mol% Pd with respect to aryl halide), DMF (12 mL) and H₂O (4 mL) were mixed in the flask, then the reaction proceeded at 120 °C under refluxing. Throughout the process, 0.2 mL mixture were pipetted every 30 min, filtered by a Nylon 66 filter (3 mm × 0.22 μm) and analyzed by gas chromatograph (Agilent 7890A) equipped with a FID and a Agilent J&K HP-5 capillary column (5% phenyl polysiloxane, 30 m × 0.25 mm × 0.25 μm). After 1 min at 70 °C, the column chamber was heated from 70 °C to 150 °C with a heating rate of 20 °C/min and kept for 1 min, then heated to 275 °C at a heating rate of 25 °C/min and kept for 3 min. The catalytic activity of the catalyst was evaluated on the basis of turnover frequency (TOF, moles of aryl halide converted per moles of Pd per hour). After completion of the reaction, the catalyst was magnetically separated from the mixture. The filtrate was extracted by ethyl acetate. The organic phase was thoroughly washed with saturated NaCl solution several times and dried by anhydrous Na₂SO₄, followed rotary evaporation (35 °C) to remove the solvent, and then through recrystallization to obtain the products which were identified by ¹H and ¹³C NMR spectra (see ESI).

3.1 The crystal Structure, composition and morphology

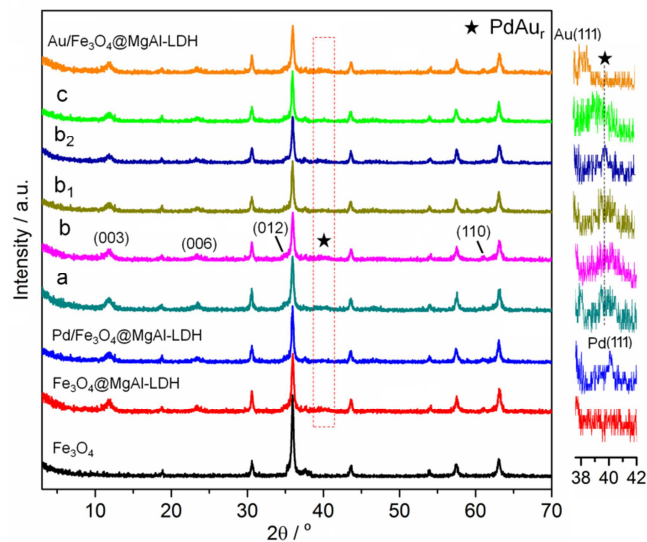


Fig. 1 XRD patterns of 1.0-PdAu_{0.11}/Fe₃O₄@LDH (a), x-PdAu_{0.16}/Fe₃O₄@LDH (x = 1.0 (b), 0.5 (b₁) and 0.1 (b₂)), 1.0-PdAu_{0.48}/Fe₃O₄@LDH (c), Pd/Fe₃O₄@LDH, Au/Fe₃O₄@LDH, the support Fe₃O₄@LDH and Fe₃O₄.

Fig. 1 shows the XRD patterns of a series of magnetic catalysts x-PdAu_r/Fe₃O₄@LDH (x = 1.0, 0.5 and 0.1 wt% of Pd, r = 0.11, 0.16 and 0.48) compared to monometallic catalysts, the support Fe₃O₄@LDH and Fe₃O₄. The Fe₃O₄ sample shows intense diffractions indexed to (111), (220), (311), (400), (422), (511) and (440) planes of *fcc* magnetite (JCPDS 19-0629), and the particle size from Debye-Scherrer formula on (311) line is 27.7 nm (Table S1), close to the critical dimension of the single magnetite domains (~30 nm) [30], implying superparamagnetic characteristic of the prepared Fe₃O₄. For the series of catalysts and the support, besides the sharp lines of Fe₃O₄ phase, a series of weak but clear lines at ~11.3° (003), 22.8° (006), 34.7° (012) and 60.6° (110) are observed [31], which can be indexed to typical *hcp* carbonate-LDH phase. Notably, the intensity ratio of *I*₁₁₀/*I*₀₀₃ for Fe₃O₄@LDH is 0.71, clearly larger than those of pure LDH of 0.26 (Table S1), suggesting the oriented growth of LDH with *ab*-face vertical to the surface of Fe₃O₄ core [25,26]. Noted that the XRD lines of all the x-PdAu_r/Fe₃O₄@LDH catalysts clearly show a weak single peak of PdAu crystallites (enlarged patterns in Fig. 1) at 2θ located between the peak positions of Au(111) (38.2°) (JCPDS 04-0784) and Pd(111) (40.1°) (JCPDS 46-1043), implying the formation of highly dispersed PdAu nanoalloys in the obtained catalysts.

The FTIR spectra of the catalysts x-PdAu_r/Fe₃O₄@LDH compared to the support (Fig. S1) show broad and strong absorption at ~3450 cm⁻¹ due to the hydroxyl stretching vibration rising from M-OH groups on the LDH nanoplates [31,32]. A sharp absorption at 1379 cm⁻¹ and a weak one at 868 cm⁻¹ can be assigned to the ν₃ (asymmetric stretching) and ν₂ (out-of-plane deformation) modes of CO₃²⁻ ions, respectively [32]. While a peak at ~428 cm⁻¹ (not shown in Fe₃O₄) can be assigned to the M-O lattice mode of LDH [22,33], and the sharp band at 584 cm⁻¹ to the Fe-O mode of Fe₃O₄ [27]. These observations clearly imply the well-defined assembly of CO₃²⁻-LDH and Fe₃O₄ phase. As for weak bands at 2923 and 2853 cm⁻¹ of all the catalysts, they can be ascribed to the ν_{as} and ν_s modes of -CH₂ of PVP molecules [32,34]. While a strong band at 1648 cm⁻¹ assigned to C=O of PVP clearly downshifts compared to pure PVP (1680 cm⁻¹), ascribing to the chemisorption of PVP on PdAu alloy

nanocrystallites through O atom of C=O group weakening the C=O bond [34].

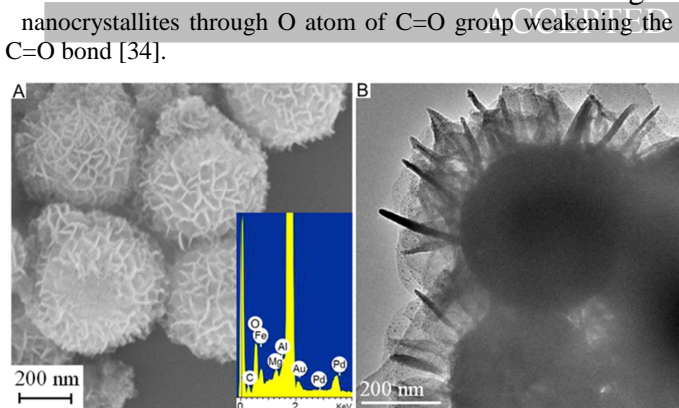


Fig. 2 SEM (A) and TEM (B) image of the catalyst 1.0-PdAu_{0.16}/Fe₃O₄@LDH, insets: EDS.

Fig. 2 shows the SEM (A) and TEM (B) image of the catalyst 1.0-PdAu_{0.16}/Fe₃O₄@LDH, while those of other catalysts x-PdAu_r/Fe₃O₄@LDH, 1.0-PdAu_{0.16}/LDH, the support Fe₃O₄@LDH and Fe₃O₄ are given in Fig. S2. Fig. S2A clearly shows nearly monodispersed microspheres of Fe₃O₄ with a smooth surface and a mean diameter of 526 ± 32 nm. After coating with LDH, Fe₃O₄@LDH (Fig. S2B) clearly shows a honeycomb-like morphology holding many voids with size of 25–70 nm, and interestingly, the LDH nanoplates with the dimensions of ~200 × 20 nm grow preferably in the orientation of *c*-axis parallel to and *ab*-face vertical to the surface of Fe₃O₄ core, and its TEM image (insets in Fig. S2B) shows typical core@shell structure. Moreover, there is no aggregation of single LDH plates (Fig. S2G) in this structure, implying that Fe₃O₄ core can greatly suppress the particle–particle interactions often occurred among the LDH nanoparticles [35]. The SEM images of the magnetic catalysts (Fig. 2A and Fig. S2(C-F)) all show similar morphology to its support, which is quite different from the aggregation of pure LDH supported PdAu catalyst (Fig. S2G) and may be in favor of the exposure of the active sites.

Fig. 3 shows the HRTEM of the x-PdAu_r/Fe₃O₄@LDH catalysts, while those of monometallic catalysts are shown in Fig. S3. The Pd particle size of monometallic Pd/Fe₃O₄@LDH catalyst ranges from 1 to 7 nm with mean size of 2.00 ± 0.42 nm, clearly illustrating the heterogeneity of size of mono-Pd catalyst (Fig. S3a). As for monometallic Au/Fe₃O₄@LDH prepared by the same method, it shows obviously aggregated and much larger Au particles (> 20 nm) (Fig. S3b), similar to Ebitani's result [29], while another one Au/Fe₃O₄@LDH-1 prepared by Au nanoclusters precursor method depicts well-dispersed Au nanoparticles of 4.26 ± 0.96 nm (Fig. S3c). After alloying with Au, the PdAu catalysts 1.0-PdAu_r/Fe₃O₄@LDH (*r* = 0.11, 0.16 and 0.48) (insets in Fig. 3a, b and c) present obviously homogeneous dispersion of metal nanoclusters, with mean sizes of 2.35 ± 0.47, 1.81 ± 0.33 and 2.55 ± 0.49 nm, respectively, clearly smaller than 1.0-PdAu_{0.16}/LDH (2.87 ± 0.50 nm in Fig. S2H), and the 1.0-PdAu_{0.16}/Fe₃O₄@LDH has the minimum PdAu NCs' size and the narrowest size distribution (1.0 – 3.0 nm). These results strongly demonstrate that size and size distribution of PdAu NCs can be tuned effectively by incorporating appropriate amount of gold. Further reducing Pd loading with Au/Pd ratio of 0.16, the obtained x-PdAu_{0.16}/Fe₃O₄@LDH (*x* = 0.5 and 0.1) (Fig. 3b₁ and b₂) exhibit further reduced NCs' sizes of 1.75 ± 0.40 and 1.70 ± 0.30 nm, respectively, indicating that the Pd loadings has a slight effect on the size and size distribution of PdAu NCs.

The magnified HRTEM images of the series of catalysts x-PdAu_r/Fe₃O₄@LDH clearly show that the PdAu NCs are tightly anchored on the margin of LDH nanosheets (arrows marked in Fig. 3a'–c') or embedded deeply into LDH laminate, implying

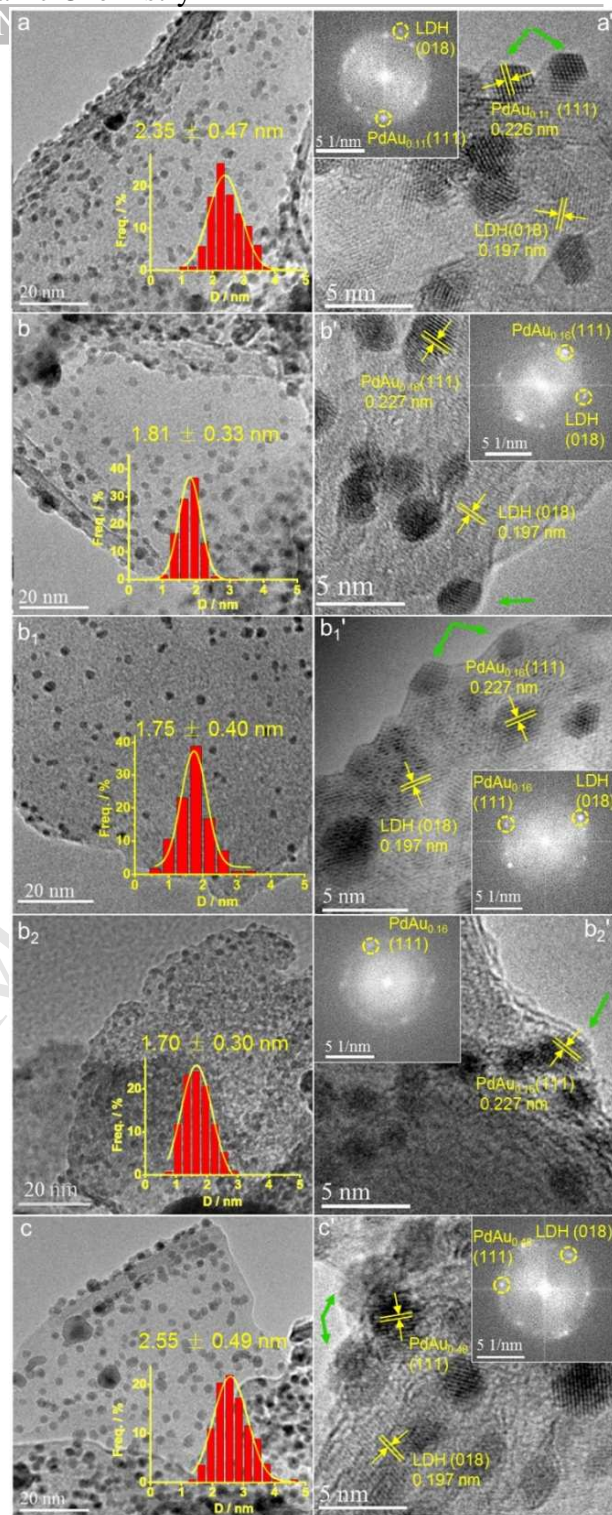


Fig. 3 The low- and high-magnified HRTEM images of 1.0-PdAu_{0.11}/Fe₃O₄@LDH (a, a'), x-PdAu_{0.16}/Fe₃O₄@LDH (*x* = 1.0 (b, b'), 0.5 (b₁, b₁') and 0.1 (b₂, b₂') and 1.0-PdAu_{0.48}/Fe₃O₄@LDH (c, c') (insets: histograms of particle size distribution and FFT).

possibly strong interaction between PdAu NCs and the support. The lattice spacings for PdAu nanocrystallites of the 1.0-PdAu_r/Fe₃O₄@LDH (*r* = 0.11, 0.16 and 0.48) are 0.226, 0.227 and 0.229 nm, respectively, in line with FFT images (insets in Fig. 3a'–c'), which are between the values of bulk Pd(111) (0.225 nm, JCPDS 46-1043) and bulk Au(111) (0.235 nm, JCPDS 04-0784), indexed to the (111) planes of the PdAu alloy phase and consistent with the *d*-spacing calculated from Vegard's law [36]. Moreover, (018) lattice fringes of the shell LDH can

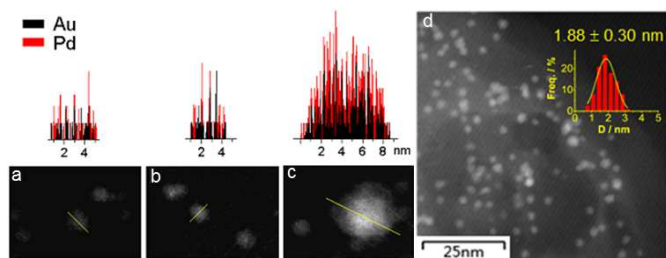


Fig. 4 The line profiles of EDS spectra from HAADF-STEM for the specially selected PdAu NCs on the 1.0-PdAu_{0.11}/Fe₃O₄@LDH (a), 1.0-PdAu_{0.16}/Fe₃O₄@LDH (b), 1.0-PdAu_{0.48}/Fe₃O₄@LDH (c) and STEM image of 1.0-PdAu_{0.16}/Fe₃O₄@LDH (d) with particle size distribution.

also be found in the HRTEM images with corresponding diffraction dots in FFT images. The HAADF-STEM and STEM-EDS analyses of the specially selected PdAu NCs in three PdAu alloy catalysts (larger particles selected for instrument's detection limitations) (Fig. 4a-c) demonstrate that the NCs consist of both Pd and Au, which indicate forcefully that the Pd and Au coexist in the form of alloy state in the catalysts as XRD and HRTEM indicated. For 1.0-PdAu_{0.16}/Fe₃O₄@LDH, the point analyses of the randomly selected NCs also verify that most of obtained NCs contain both Pd and Au, and only a very few fraction are pure Pd, as also evidenced by the mostly spatial coincidence of the Au and Pd in EDS mapping analysis (Fig. S4). The quantitative analysis of the EDS profile shows that the catalyst is composed of mixed Au and Pd atoms with *r* of 0.18, in good agreement with the ICP data (0.16). Moreover, the particle size distribution from STEM of 1.0-PdAu_{0.16}/Fe₃O₄@LDH (Fig. 4d) gives the mean size of 1.88 ± 0.30 nm, in line with the HRTEM data.

The BET analyses show that the catalysts 1.0-PdAu_{*r*}/Fe₃O₄@LDH (*r* = 0.11, 0.16 and 0.48) possess similar specific surface areas of 49.9-52.9 m² g⁻¹ to the support Fe₃O₄@LDH (53.1 m² g⁻¹) (Fig. S5 and Table S2) and typical mesoporosity with mean pore sizes of 2.1-2.7 nm, along with the hierarchical core@shell structure with abundant accessible edge and junctions as SEM indicated, being in favor of the exposure of catalytic active sites [26].

3.2 Magnetic property

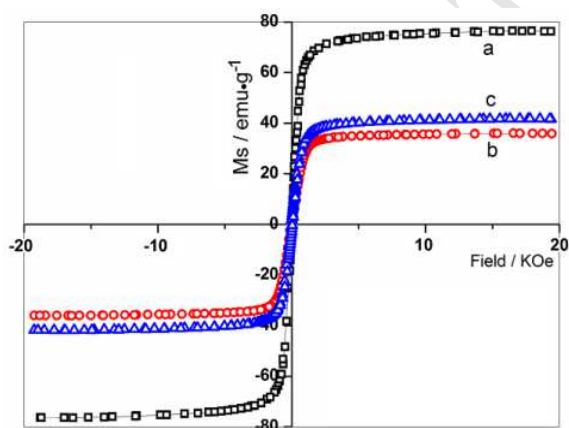


Fig. 5 The magnetization curves of Fe₃O₄ (a), Fe₃O₄@LDH (b) and the catalyst 1.0-PdAu_{0.16}/Fe₃O₄@LDH (c).

Fig. 5 depicts the magnetization curves of the catalyst 1.0-PdAu_{0.16}/Fe₃O₄@LDH compared with the support Fe₃O₄@LDH and Fe₃O₄. The magnetization curves of the three samples exhibit typically superparamagnetic characteristics, also verified by their weak coercive force and remanence, in line with the *D*₃₁₁ value of the magnetic core Fe₃O₄. The 1.0-PdAu_{0.16}/Fe₃O₄@LDH and support exhibit considerable saturation magnetization (*M*_s) of

36.1 and 41.8 emu·g⁻¹, respectively, though lower than Fe₃O₄ (76.5 emu·g⁻¹) owing to the coating of nonmagnetic shell LDH [25,26]. Consequently, the obtained magnetic core@shell catalysts are easily separated from reaction system by using an external magnet.

3.3 Catalytic performance

The Heck reaction of iodobenzene (PhI) with styrene is selected as a probe reaction to study the catalytic performance of the magnetic catalysts. The 1.0-PdAu_{0.48}/Fe₃O₄@LDH is first employed to optimize Heck reaction conditions involving solvent composition and additive base type (since pure PdAu_{0.48}-PVP colloid or Fe₃O₄@LDH without base additive shows no product), and the results are summarized in Table S3. The volume ratio of DMF and H₂O is adjusted to explore the suitable solvent composition, and the best yield (87.9%) is obtained in the case of *v*_{DMF}:*v*_{H₂O} = 3:1 at 2 h (Table S3, entry 2), while the lower or even no yield is detected under other solvent compositions. Moreover, the weak base K₂CO₃ is found to be the preferred choice for the reaction to both the stronger base NaOH and weaker bases (NaAc and N(C₂H₅)₃) upon the highest selectivity and yield for the Heck reaction (Table S3, entries 2, 6–8). Therefore, the optimized reaction condition using K₂CO₃ as base additive and DMF-H₂O with *v/v*=3:1 as solvent is achieved.

Then, the effect of Au/Pd ratios on the Heck reaction is studied over the series of magnetic PdAu alloy NCs catalysts 1.0-PdAu_{*r*}/Fe₃O₄@LDH under the optimized reaction conditions (Table 1). Not surprisingly, monometallic Au/Fe₃O₄@LDH-1 shows no activity, while the Pd/Fe₃O₄@LDH presents high activity with the Yield of 81.8% in 2 h, clearly indicating that Pd species are the intrinsic active sites for the Heck reaction as previously reported [1,2]. However, after alloying with Au, three alloy catalysts 1.0-PdAu_{*r*}/Fe₃O₄@LDH (*r* = 0.11, 0.16 and 0.48) all show higher activity than the Pd/Fe₃O₄@LDH. Especially, the 1.0-PdAu_{0.16}/Fe₃O₄@LDH with smallest PdAu NCs' size (~1.81 nm) exhibits the highest activity with the Yield of 87.6% in 1 h. These results strongly suggest that Au/Pd ratios can greatly influence the catalytic performance of the magnetic catalysts 1.0-PdAu_{*r*}/Fe₃O₄@LDH for the Heck reaction. It is also noted that under no base additive, 1.0-PdAu_{0.48}/Fe₃O₄@LDH shows quite low yield (4%) at 2 h but increased to 53.5% at 9 h (Table S3, entry 9), implying that the magnetic support with intrinsic basic LDH layers serves to the base-required Heck reaction to some extent.

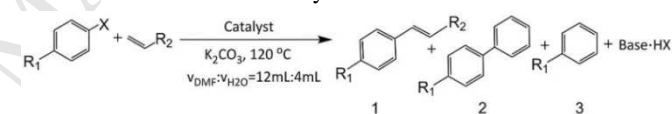
Furthermore, the effect of the Pd loadings of the magnetic PdAu NCs catalysts on the Heck reaction is studied (Table 1). The low Pd-loading samples *x*-PdAu_{0.16}/Fe₃O₄@LDH (*x* = 0.5 and 0.1) exhibit the Yield of 94.1% in 2.0 h and 89.9% in 1.5 h with Pd dosage of 0.05 mol% respectively, while 1.0-PdAu_{0.16}/Fe₃O₄@LDH is 94.0% in 3.5 h. However, further reduced Pd loading sample 0.05-PdAu_{0.16}/Fe₃O₄@LDH show decreased Heck activity probably due to their sequentially reduced active sites. The above results clearly demonstrate that the catalyst 0.1-PdAu_{0.16}/Fe₃O₄@LDH possesses even higher Heck coupling activity, implying the predominant size effect of the present magnetic PdAu alloy NCs catalysts. Actually, the catalyst 0.1-PdAu_{0.16}/Fe₃O₄@LDH presents much better Heck reactivity, even at lower temperature with stilbene yield of 92.3% at 90 °C, than previously reported magnetic Fe₃O₄/SiO₂/HPG-Pd, [21] Fe₃O₄@SiO₂-Dendrimer-Pd [23], Pd-MNPSS (magnetic NPs–starch substrate) [37] and Fe₃O₄@PUNP (Poly (undecylenic acid-co-N-isopropylacrylamide-co-potassium 4-acryloxyoyl-pyridine-2, 6-dicarboxylate))-Pd [38] with complicated preparation under similar reaction conditions (Table 1).

Table 1 Catalytic activity of the various catalysts for the Heck reaction of iodobenzene with styrene. ^a

Catalysts	D _{Pd} /nm ^b	Pd/ mol%	t/h	Conv./ %	Yield/%	Ref.
1.0-PdAu _{0.11} /Fe ₃ O ₄ @LDH	2.35±0.47	0.30	0.5/1.5	39.9/92.1	36.0/86.1	This work
1.0-PdAu _{0.16} /Fe ₃ O ₄ @LDH	1.81±0.33	0.30	0.5/1.0	50.6/92.9	45.8/87.6	This work
1.0-PdAu _{0.16} /Fe ₃ O ₄ @LDH	1.81±0.33	0.05	0.5/3.5	16.0/99.5	15.0/94.0	This work
0.5-PdAu _{0.16} /Fe ₃ O ₄ @LDH	1.75±0.40	0.05	0.5/2.0	30.1/99.9	27.9/94.1	This work
0.1-PdAu _{0.16} /Fe ₃ O ₄ @LDH	1.70±0.30	0.05	0.5/1.5	31.1/93.0	28.2/89.9	This work
0.1-PdAu _{0.16} /Fe ₃ O ₄ @LDH ^c	1.70±0.30	0.05	0.5/3.0	22.4/96.4	22.0/92.3	This work
1.0-PdAu _{0.48} /Fe ₃ O ₄ @LDH	2.55±0.49	0.30	0.5/2.0	28.0/91.6	25.9/87.9	This work
1.0-PdAu _{0.16} /LDH	2.87±0.50	0.30	0.5/1.0	13.5/39.5	12.7/37.6	This work
Pd/Fe ₃ O ₄ @LDH	2.00±0.42	0.30	0.5/2.0	21.0/86.8	19.3/81.8	This work
Au/Fe ₃ O ₄ @LDH-1	4.26±0.96	0.30	0.5/4.0	n.d.	n.d.	This work
0.05-PdAu _{0.16} /Fe ₃ O ₄ @LDH	-	0.05	0.5/4.0	12.6/90.7	12.6/88.9	This work
Fe ₃ O ₄ /SiO ₂ /HPG-Pd ^d	-	3.0	6.0	-	93	21
Fe ₃ O ₄ @SiO ₂ -Dendrimer-Pd ^e	-	0.009	2.0	-	92	23
Pd-MNPSS ^f	-	0.36	4.0	-	90	37
Fe ₃ O ₄ @PUNP-Pd ^g	-	0.1	8.0	-	95	38

^a Reaction conditions: PhI (1 mmol), styrene (1.5 mmol), v_{DMF}:v_{H₂O} = 12 mL:4 mL, K₂CO₃ (3 mmol), 120 °C, catalysts x-PdAu_r/Fe₃O₄@LDH under atmospheric conditions. ^b Mean values upon 200 individual NCs in TEM images. ^c PhI (50 mmol), styrene (75 mmol), v_{DMF}:v_{H₂O}=120 mL:40 mL, K₂CO₃ (100 mmol), 90 °C. ^d PhI (0.1 mmol), styrene (0.2 mmol), DMF (8 mL), NaAc (0.18 mmol), 140 °C. ^e PhI (1 mmol), styrene (2 mmol), DMF (2 mL), Et₃N (3 mmol), 120 °C. ^f PhI (1 mmol), styrene (1.2 mmol), H₂O (5 mL), K₂CO₃ (2.0 mmol), 100 °C. ^g PhI (1 mmol), styrene (1.5 mmol), v_{H₂O}:v_{DMF} = 1 mL:1 mL, K₂CO₃ (3 mmol), Ar atmosphere, 94 °C.

To verify the universal adaptability of the present PdAu NCs catalysts x-PdAu_r/Fe₃O₄@LDH for the Heck reaction, the range of aryl halides and alkenes is explored over the catalyst 0.1-PdAu_{0.16}/Fe₃O₄@LDH under the optimal reaction conditions (Table 2). The catalyst exhibits excellent catalytic performance for the Heck reaction of aryl iodides with electron-withdrawing groups or electron-donating groups and styrene, to give the desired Heck reaction products 1a-1e in 89.7–99.9% yield (Table 2, entries 1–5). PhI reacts with methyl acrylate and ethyl acrylate, to give 1f in 99.1% yield and 1g in 99.0% yield, respectively (Table 2, entries 6 and 7). As for the reaction of 4-PhI-OH and 4-PhI-CHO with styrene, instead of Heck product but an Ullmann reaction product 2 in 98.0% yield (Table 2, entry 8) and a hydrogenation product 3 in 99.3% yield (Table 2, entry 9) are obtained, respectively. Then for the reaction of bromobenzene with styrene and ethyl acrylate, which give the Heck product 1c in 92.2% yield and 1g in 92.4% yield, respectively (Table 2, entries 10 and 11). While the reaction of 4-PhBr-CHO with styrene gives the Heck product 1h in 87.7% yield along with hydrogenation product 3 in 12.1% yield (Table 2, entry 12), and the reaction of 4-PhBr-OH with styrene gives the Heck product 4-hydroxystilbene in 98.6% yield (Table 2, entry 13), probably attributed to the different dissociation energy of C-I and C-Br bond. These results are much higher than those of previously reported catalyst SiNA-Pd (SiNA: silicon nanowire array) [39] (Yield: 82%, 48.0 h) and Pd(2.5)/NT (NT: hydrogen titanate nanotubes) [40] with lower Heck product yield (43.2%, 24.0 h), and higher than those of Pd@Co/CNT-50 (Yield: 88%, 6 h) [41] under similar catalytic reaction conditions (Table 2, entries 14–16), implying the higher Heck activities of the present 0.1-PdAu_{0.16}/Fe₃O₄@LDH for aryl bromides and alkenes. The above results clearly demonstrate that the present magnetic PdAu alloy NCs catalysts x-PdAu_r/Fe₃O₄@LDH possess an extensive substrate adaptability.

Table 2 Catalytic activity of the 0.1-PdAu_{0.16}/Fe₃O₄@LDH for the Heck reaction of varied aryl halides with varied alkenes. ^a

No.	Substrate			t/h	Conv. / %	product ^b
	X	R ₁	R ₂			
1	I	NO ₂	Ph	0.67	99.9	1a (99.9)
2	I	COCH ₃	Ph	1.5	96.9	1b (95.9)
3	I	H	Ph	1.5	93.0	1c (89.7)
4	I	CH ₃	Ph	1.67	99.9	1d (96.4)
5	I	OCH ₃	Ph	2.0	90.7	1e (90.3)
6	I	H	CO ₂ CH ₃	1.5	99.6	1f (99.1)
7	I	H	CO ₂ C ₂ H ₅	1.5	99.0	1g (99.0)
8	I	OH	Ph	1.0	98.1	2 (98.0)
9	I	CHO	Ph	2.0	99.5	3 (99.3)
10	Br	H	Ph	10	95.0	1c (92.2)
11	Br	H	CO ₂ C ₂ H ₅	7.0	93.3	1g (92.4)
12	Br	CHO	Ph	2.5	99.8	1h (87.7), 3 (12.1)
13	Br	OH	Ph	12	98.9	98.6
14 ^c	Br	H	CO ₂ C ₄ H ₉	48	-	82
15 ^d	Br	H	Ph	6.0	-	88
16 ^e	Br	H	Ph	24	-	43

^a Reaction conditions: 0.1-PdAu_{0.16}/Fe₃O₄@LDH (0.05 mol% Pd), aryl halide (1.0 mmol), alkene (1.5 mmol), v_{DMF}:v_{H₂O}=12 mL:4 mL, K₂CO₃ (3.0 mmol), 120 °C. ^b The varied products were identified by ¹³C and ¹H NMR (see ESI) and the data in parentheses are yield of corresponding product by GC. ^c PhBr, butyl acrylate, NaAc, TBAB. ^d PhBr, styrene, Et₃N, DMF, N₂. ^e PhBr-CHO, styrene, Et₃N, DMF, tri-(o-tolyl)phosphine, N₂.

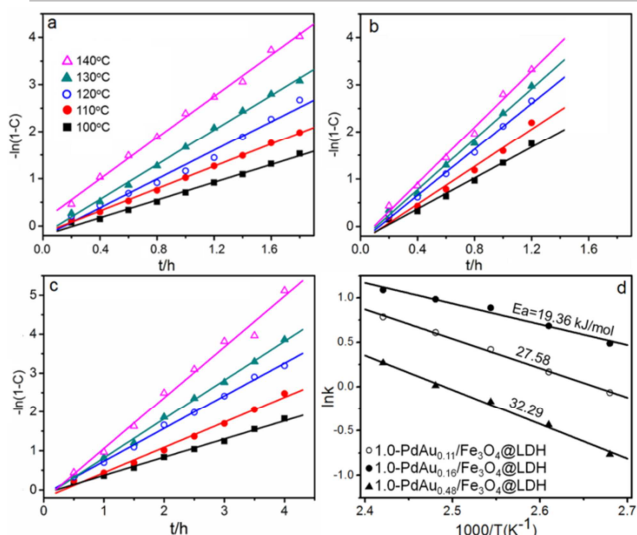


Fig. 6 $-\ln(1-C)$ against time (a-c) and Arrhenius plots (d) for the Heck reaction over 1.0-PdAu_r/Fe₃O₄@LDH ($r = 0.11$ (a), 0.16 (b) and 0.48 (c)) at temperatures of 100, 110, 120, 130 and 140 °C. Reaction conditions: catalyst (Pd: 0.3 mol% based on PhI), PhI (1.0 mmol), styrene (1.5 mmol), $v_{\text{DMF}}:v_{\text{H}_2\text{O}} = 12 \text{ mL}:4 \text{ mL}$, K_2CO_3 (3.0 mmol).

To reveal the nature reasons for different Heck reaction performance of the series of magnetic PdAu alloy nanoclusters catalysts, the macroscopic kinetic experiment of the obtained 1.0-PdAu_r/Fe₃O₄@LDH catalysts including the effect of the different Au/Pd ratios and reaction temperatures (100, 110, 120, 130 and 140 °C) on the Heck reaction rate of PhI with styrene was studied. As shown in Fig. S6, the Conv.-time (t) plots are linearly up to ca. 60% Conv. of PhI, implying that the product inhibition is very small. It can be clearly seen in Fig. 6a-c that the term $-\ln(1-C)$ is linearly increased with the reaction time for three catalysts 1.0-PdAu_r/Fe₃O₄@LDH ($r = 0.11, 0.16$ and 0.48), fitting quite well to the first order with respect to PhI. The rate constant, k , is calculated upon the slope of the $-\ln(1-C)$ verse t plot. The k values (Table S5) of the Heck reaction of PhI with styrene for three catalysts at the same temperature are found to be in an order of 1.0-PdAu_{0.16}/Fe₃O₄@LDH > 1.0-PdAu_{0.11}/Fe₃O₄@LDH > 1.0-PdAu_{0.48}/Fe₃O₄@LDH.

A good linear relationship is achieved by plotting of $\ln k$ verse $1/T$ (T : temperature), and the apparent activation energy (E_a) is calculated upon the slope by the least-square fit analysis (Fig. 6d and Table S4). The catalyst 1.0-PdAu_{0.16}/Fe₃O₄@LDH shows the lowest E_a of 19.36 kJ/mol among the three catalysts with an order of 1.0-PdAu_{0.16}/Fe₃O₄@LDH < 1.0-PdAu_{0.11}/Fe₃O₄@LDH (27.58) < 1.0-PdAu_{0.48}/Fe₃O₄@LDH (32.29). The highest k and the lowest E_a of the catalyst 1.0-PdAu_{0.16}/Fe₃O₄@LDH are consistent with its smallest PdAu NCs' size.

3.5 The structure-performance relationship.

The above results clearly suggest that the magnetic PdAu alloy nanoclusters catalysts $x\text{-PdAu}_r/\text{Fe}_3\text{O}_4@\text{LDH}$ exhibit efficiently catalytic performance for the Heck reaction. To understand and reveal the structure-performance relationship, XPS, *In situ* CO-DRIFTS and H₂-TPR analyses are performed to explore the electronic and geometric structure of the as-obtained catalysts.

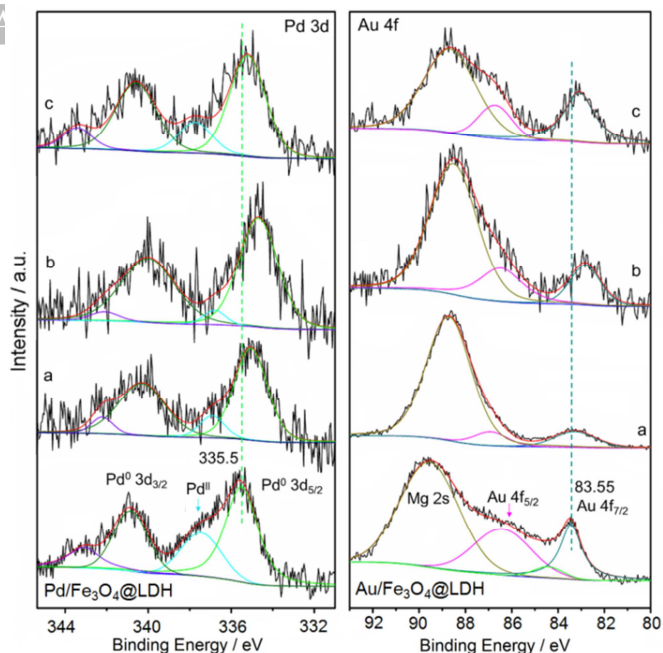


Fig. 7 Pd 3d and Au 4f XPS spectra of 1.0-PdAu_{0.11}/Fe₃O₄@LDH (a), 1.0-PdAu_{0.16}/Fe₃O₄@LDH (b), 1.0-PdAu_{0.48}/Fe₃O₄@LDH (c), Pd/Fe₃O₄@LDH and Au/Fe₃O₄@LDH.

The XPS analysis is first employed to explore the surface chemical composition and electron structure of the series of magnetic PdAu alloy NCs catalysts. The Pd 3d and Au 4f XPS spectra are shown in Fig. 7 and the corresponding parameters are listed in Table S5. The Pd 3d XPS spectrum of Pd/Fe₃O₄@LDH shows two distinct asymmetrical peaks for Pd 3d_{5/2} at binding energy (BE) of ~335.60 eV and Pd 3d_{3/2} at BE of ~341.02 eV, respectively. The deconvolution BE values of Pd 3d_{5/2} are 335.50 and 337.45 eV, which can be assigned to the Pd⁰ and Pd^{II} species, respectively [42]. The Au 4f XPS spectrum of Au/Fe₃O₄@LDH shows two asymmetrical peaks for Au 4f_{7/2} at 83.55 eV and Au 4f_{5/2} at 86.47 eV, which is overlapped by Mg 2s at 89.60 eV. The deconvolution BE values of Au 4f_{7/2} are 83.55 and 84.45 eV, attributable to surface metallic Au and Au⁺ species, respectively [42,43]. After alloying with Au, the Pd⁰ 3d_{5/2} BE values of three catalysts 1.0-PdAu_r/Fe₃O₄@LDH ($r = 0.11, 0.16$ and 0.48) are 335.05, 334.69 and 335.22 eV, with 0.45, 0.81 and 0.28 eV decrease compared with Pd/Fe₃O₄@LDH, respectively, while the Au 4f_{7/2} BE values are 83.08, 82.63 and 83.11 eV, similarly with 0.47, 0.92 and 0.44 eV decrease compared with Au/Fe₃O₄@LDH, respectively. The observed negative shift for both Pd 3d_{5/2} and Au 4f_{7/2} BE values are in line with the net charge transferring into palladium (gaining d electrons from gold) and gold (increased Au s or p electron cloud densities) [19,44], suggesting the electronic structure of the surface Pd atoms to be greatly modified by alloying with Au, besides the role of support (see later O 1s, Fe 2p, Mg 2p XPS analyses). Particularly, 1.0-PdAu_{0.16}/Fe₃O₄@LDH presents the maximum Pd⁰ 3d_{5/2} downshift, corresponding to the most negatively charged Pd⁰, that is the largest electron density of surface Pd⁰.

Though the XPS detective depth is up to 10 nm, which is higher than the size of the PdAu alloy NCs in the obtained magnetic catalysts, the XPS data may strongly disclose the surface composition of the PdAu alloy catalysts [45,46]. As shown in Table S5, the XPS-derived Au/Pd and Pd⁰/(Pd^{II}+Pd⁰) molar ratios reveal the surface metal composition is affected by the addition of Au in the as-obtained magnetic PdAu alloy NCs catalysts. It is found that surface Au/Pd ratios of the alloy catalysts by XPS are obviously different from those of bulk ratios by ICP. In detail, the surface Au/Pd ratios of 1.0-

PdAu_{0.11}/Fe₃O₄@LDH and 1.0-PdAu_{0.16}/Fe₃O₄@LDH are 0.62 and 0.73, ca. 5.5 and 4.6 times those of the corresponding bulk ratios, respectively, while the surface Au/Pd ratio for the 1.0-PdAu_{0.48}/Fe₃O₄@LDH is only 0.22. Furthermore, the XPS-derived Pd⁰/(Pd⁰+Pd^{II}) values of three catalysts 1.0-PdAu_r/Fe₃O₄@LDH (r = 0.11, 0.16 and 0.48) upon deconvolution are 85.0%, 93.1% and 77.9%, respectively, much higher than that of Pd/Fe₃O₄@LDH (69.1%). It can be attributed to the influence of alloying with Au to various degrees, in line with the findings of Liao *et al.* [45] and Huang *et al.* [47], on the protecting Pd⁰ species from being oxidized to Pd^{II}. These results indicate that the surface metallic composition of magnetic PdAu alloy NCs catalysts can be effectively tuned by the initial Au/Pd ratio, and the 1.0-PdAu_{0.16}/Fe₃O₄@LDH has the maximum Pd⁰ percentage and Au-rich surface which might form properly isolated Pd atoms or small ensembles by Au.

To get more insight into the surface characteristics of the series of magnetic PdAu alloy NCs catalysts, O 1s, Fe 2p and Mg 2p spectra (Fig. S7) are carefully analyzed for the catalysts compared with the support and Fe₃O₄, and the parameters are listed in Table S6. The curve fittings of O 1s spectra of three catalysts 1.0-PdAu_r/Fe₃O₄@LDH (r=0.11, 0.16 and 0.48) and the support reveal that there are three oxygen species as surface OH (531–532 eV), lattice O²⁻ (520–531 eV) and adsorbed H₂O and/or intercalated carbonate (532–534 eV) species [42]. The BE values of OH group in the three catalysts all shift to higher levels compared to the support, implying that the occurrence of electron transfer from the surface OH groups related to LDH layer Mg²⁺ ions to PdAu NCs. The 1.0-PdAu_{0.16}/Fe₃O₄@LDH kept the largest fraction of M-OH (70.3%) shows the highest BE increase, suggesting the most electron transfer from M-OH to PdAu NCs, consistent with its highest Heck reactivity.

The Fe 2p XPS spectra of three PdAu alloy NCs catalysts 1.0-PdAu_r/Fe₃O₄@LDH (r = 0.11, 0.16 and 0.48) compared with Pd/Fe₃O₄@LDH, Au/Fe₃O₄@LDH and Fe₃O₄@LDH show two distinct asymmetrical peaks at ~710.40 and ~724.50 eV for Fe 2p_{3/2} and Fe 2p_{1/2}, and the deconvolution BE values of Fe 2p_{3/2} are 709.75 and 711.85 eV, 709.90 and 711.95 eV, 709.61 and 711.59 eV, 709.62 and 711.49 eV, 709.74 and 711.18 eV as well as 709.60 and 711.00 eV, which can be ascribed to the Fe²⁺ and Fe³⁺ species of Fe₃O₄ core [42], respectively. The Fe²⁺ 2p_{3/2} and Fe³⁺ 2p_{3/2} BE values of the support Fe₃O₄@LDH are 0.16 and 0.30 eV downshift from the Fe₃O₄ (709.76 and 711.30 eV), respectively. The slight BE downshift of Fe²⁺ and Fe³⁺ species in Fe₃O₄@LDH support compared to the Fe₃O₄ can be attributed to partial charge transfer from the LDH shell to Fe₃O₄ core on various electronegativity of Fe (1.83) and Mg (1.31) elements [48], in line with a slight upshift (0.18 eV) of Mg 2p (50.38 eV) of the support Fe₃O₄@LDH compared to pure LDH (50.20 eV) [28]. For the PdAu NCs catalysts 1.0-PdAu_r/Fe₃O₄@LDH (r = 0.11, 0.16 and 0.48) and Pd/Fe₃O₄@LDH and Au/Fe₃O₄@LDH, the BE values of Fe²⁺ and Fe³⁺ species show varied upshift (0.15 and 0.85 eV, 0.30 and 0.95 eV, 0.01 and 0.59 eV, 0.02 and 0.49 eV as well as 0.14 and 0.18 eV, respectively) compared to Fe₃O₄@LDH after loading PdAu alloy NCs with greater electronegative Pd (2.20) and Au (2.54) [48], while the Mg 2p BE values show negligible shift compared to the support. These observations can be attributed to partial electron transfer from Fe₃O₄ core to the LDH shell, then to PdAu alloy NCs, in line with the downshift of ~0.29 eV of Pd⁰ 3d_{5/2} and ~0.19 eV of Au 4f_{7/2} in 1.0-PdAu_{0.16}/Fe₃O₄@LDH compared to non-magnetic 1.0-PdAu_{0.16}/LDH (Fig. S8 and Table S5). The above XPS data strongly demonstrate the presence of remarkable PdAu NCs – LDH – Fe₃O₄ three-phase synergistic effect in the present magnetic PdAu alloy NCs catalysts.

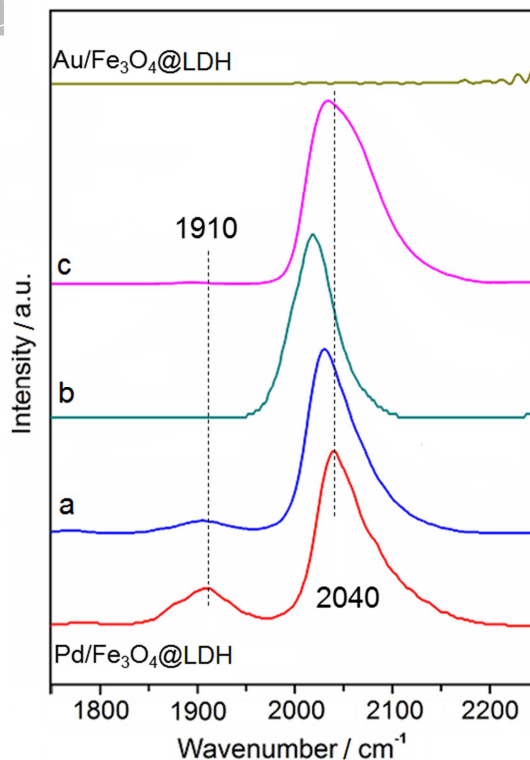


Fig. 8 *In situ* DRIFT spectra of CO adsorption on 1.0-PdAu_{0.11}/Fe₃O₄@LDH (a), 1.0-PdAu_{0.16}/Fe₃O₄@LDH (b), 1.0-PdAu_{0.48}/Fe₃O₄@LDH (c), Pd/Fe₃O₄@LDH and Au/Fe₃O₄@LDH.

In situ DRIFTS of CO adsorption is an important surface-sensitive technique to probe the geometric and electronic effects arising from the addition of a second metal, which are considered to be the key factor influencing the catalytic activity of bimetallic catalysts. Fig. 8 depicts DRIFT spectra of CO adsorption on the obtained catalysts 1.0-PdAu_r/Fe₃O₄@LDH (r = 0.11, 0.16 and 0.48) compared to Pd/Fe₃O₄@LDH and Au/Fe₃O₄@LDH. For the Au/Fe₃O₄@LDH, no band detected may be owing to the weaker CO adsorption strength [49]. However, the Pd/Fe₃O₄@LDH shows a sharp peak at ~2040 cm⁻¹ and a weak one at ~1910 cm⁻¹, which could be assigned to linear and two fold-bridged adsorbed CO on metallic Pd atoms, respectively [50,51]. After alloying with Au, the peaks of two fold-bridged adsorbed CO on Pd of the three PdAu alloy NCs catalysts almost disappear. The peak area ratios of linear adsorbed CO (A_l) to total of linear and two fold-bridged CO (A_t) are 93.9%, 100% and 99.7% for the three catalysts with r of 0.11, 0.16 and 0.48, respectively, obviously higher than that of Pd/Fe₃O₄@LDH (83.1%). These results illustrate that the magnetic PdAu alloy NCs catalysts are preferred to adsorb CO molecules in linear pattern, and the 1.0-PdAu_{0.16}/Fe₃O₄@LDH presents the largest A_l/A_t value probably originating from isolated Pd atoms or small ensembles by Au doping, which are favorable for the Heck reaction [50]. It is noted that the linear adsorbed CO bands on Pd at 2033, 2015 and 2030 cm⁻¹ of the three catalysts 1.0-PdAu_r/Fe₃O₄@LDH (r = 0.11, 0.16 and 0.48) show remarkable redshift of 7, 25 and 10 cm⁻¹, respectively, compared to Pd/Fe₃O₄@LDH, suggesting the increased electron density of the surface Pd atoms via alloying with Au. Particularly, 1.0-PdAu_{0.16}/Fe₃O₄@LDH exhibits the maximum redshift, corresponding to the most negatively charged Pd⁰, in line with the XPS data, which explains its best Heck activity from the electronic effect. The above analyses strongly illustrate that alloying Pd with Au can greatly influence the geometric structure (the added Au isolates the continuous Pd sites) and electronic structure (neighboring Au atoms increase the electron density of Pd) of the present PdAu alloy NCs catalysts.

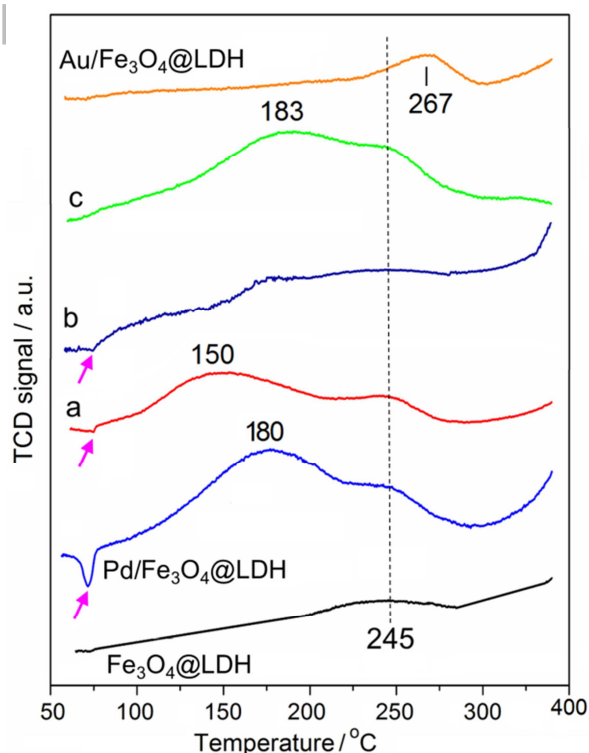


Fig. 9 H₂ TPR of 1.0-PdAu_{0.11}/Fe₃O₄@LDH (a), 1.0-PdAu_{0.16}/Fe₃O₄@LDH (b), 1.0-PdAu_{0.48}/Fe₃O₄@LDH (c), monometallic catalysts, and the support Fe₃O₄@LDH.

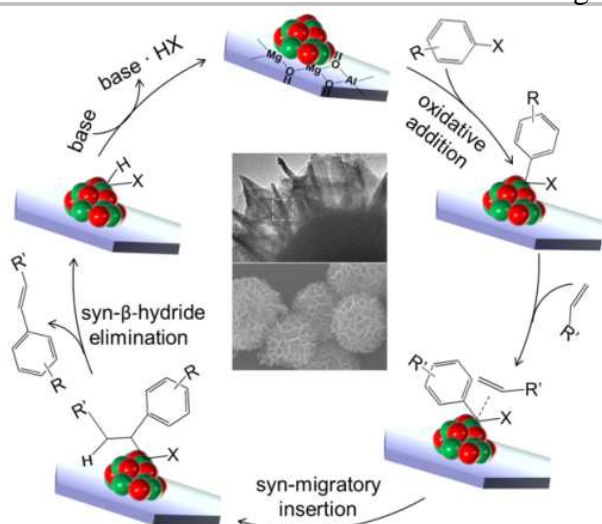
Fig. 9 presents H₂ TPR of the PdAu alloy NCs catalysts 1.0-PdAu_r/Fe₃O₄@LDH ($r = 0.11, 0.16$ and 0.48) compared to Pd/Fe₃O₄@LDH, Au/Fe₃O₄@LDH, and Fe₃O₄@LDH. The monometallic Au/Fe₃O₄@LDH only shows a weak broadened hydrogen consumption peak at 267 °C, which may be ascribed to reduction of Au⁺ to Au⁰ species [52], implying the presence of small amount of Au⁺ state, in line with the XPS data. The Pd/Fe₃O₄@LDH displays a single negative peak at 72 °C resulting from dissociation of β-Pd hydride formed by the hydrogen adsorbing on Pd⁰ when the pressure of hydrogen surpasses 0.02 atm [45,53], and a strong broad hydrogen consumption peaks at 180 °C with H₂ consumptions of 30 μmol/g attributed to the reduction of Pd^{II} to Pd⁰ [45]. The broad shoulder at 245 °C can be ascribed to the reduction of the ferric species on the magnetic support, which occurred at much lower temperature than normally expected (350 – 950 °C) [54–56], ascribed to that Pd⁰ species resulted from initial reduction facilitates dissociative chemisorption of H₂ which has enough reducibility for the ferric species [57]. After alloying with Au, the catalysts 1.0-PdAu_r/Fe₃O₄@LDH show negative peaks around 75 °C with a slight shift compared with the monometallic Pd/Fe₃O₄@LDH, and the peak gradually weakens with increasing Au/Pd ratio and even disappears at $r = 0.48$. The two catalysts 1.0-PdAu_r/Fe₃O₄@LDH with $r = 0.11$ and 0.48 show H₂ consumption peaks owing to the reduction of Pd^{II} to Pd⁰ at varied temperatures of 150 and 183 °C, with lower H₂ consumptions of 17 and 23 μmol/g than Pd/Fe₃O₄@LDH, respectively, suggesting various interactions occurring between Pd and the added Au. However, the catalyst 1.0-PdAu_{0.16}/Fe₃O₄@LDH displays a very weak H₂ consumption peak at ~180 °C with much lower H₂ consumption (4.7 μmol/g) corresponding to its lowest Pd²⁺ fraction (XPS indicated) associated with its proper Au doping protecting Pd⁰ species from being oxidized to Pd^{II} and stronger Pd-Au interaction.

The above results strongly demonstrate that the catalyst 1.0-PdAu_{0.16}/Fe₃O₄@LDH possesses the most negatively charged Pd⁰, the maximum Pd⁰ percentage and Au-rich surface and the

strongest PdAu_r NCs–LDH–Fe₃O₄ three-phase synergistic effect along with its smallest PdAu alloy NCs' size, thus afford to its best Heck reaction activity.

In order to study whether the catalytic mechanism of the catalysts x -PdAu_r/Fe₃O₄@LDH follow a homogeneous or heterogeneous catalysis path, the hot filtration experiments are performed [11,50]. In detail, two parallel tests are realized for the Heck reaction of PhI with styrene on the catalyst 1.0-PdAu_{0.16}/Fe₃O₄@LDH (Pd: 0.3 mol%) under the optimized reaction condition. The first test proceeds until the reaction is completed. After separating catalyst from the reaction system by an NdFeB magnet, ICP analysis of the filtrate shows that only 0.01 ppm (corresponding to 0.05 wt% of the initial amount) Pd leached into the solution at the end of reaction. The second test is stopped after 0.4 h with PhI Conv. of 47.2%. After magnetic separation, the ICP analysis of the filtrate shows that 0.30 ppm (1.5 wt% of the initial amount) Pd leached into the solution. The reaction is continued for an additional 1.2 h with the filtrate, and the PhI Conv. almost remains constant. These results verify that only Pd bound to the Fe₃O₄@LDH support during the reaction is active, and the Heck reaction occurs on the heterogeneous surface of the present magnetic PdAu alloy nanoclusters catalysts.

On the basis of all the Heck reaction results and related catalysts characterization data along with previous findings [2,11], we tentatively propose a possible Heck coupling mechanism of aryl halides (Ar-X) with alkenes on the present magnetic PdAu alloy NCs catalysts as shown in Scheme 2. Firstly, the PdAu alloy NCs undergo oxidative addition with aryl halides to form a surface transient organometallic intermediate (STOI) Ar-PdAu_r-X/Fe₃O₄@LDH, as is evident from XPS and TGA-DTA-MS on the intermediate. The Pd 3d, I 3d and C 1s XPS spectra of a typical STOI CH₃Ph-PdAu_{0.16}-I/Fe₃O₄@LDH (experimental details see ESI) are shown in Fig. S9. The Pd 3d XPS spectrum of the STOI shows two broaden overlapping peaks for Pd 3d_{5/2} at ~336.02 eV and Pd 3d_{3/2} at ~339.85 eV. The deconvolution of Pd 3d_{5/2} XPS gives 335.00 eV assigned to Pd⁰ and 337.02 eV to Pd^{II}, featured as higher BE values ($\Delta E = -0.2$ eV) and much higher Pd^{II} proportion (45.5%) than the fresh one (6.9%), resulting from the presence of the Pd-I in the formed STOI [11]. The I 3d XPS shows two sharp peaks for I 3d_{5/2} at 618.96 and I 3d_{3/2} at 630.36 eV, respectively, assigned to the Pd-I bond [43]. The C 1s XPS shows two lines at 284.99 and 288.36 eV, which may be assigned to a carbon impurity and Pd-C, respectively [11]. The TGA-DTA-MS study of CH₃Ph-PdAu_{0.16}-I/Fe₃O₄@LDH gives m/z values of 91 and 127 amu corresponding to CH₃Ph and iodide species, respectively (Fig. S9), while the m/z signal corresponding to CH₃-PhI cannot be detected, indicating that the pyrolysis products are obtained from this intermediate. The above results further demonstrate that the Heck reaction indeed occurs on the heterogeneous surface of the magnetic PdAu alloy NCs catalysts. It should be mentioned that at this stage, both the neighboring Au atoms and the hierarchical structured Fe₃O₄@LDH support contribute to the increase of the electronic density of Pd centers to facilitate the oxidative addition of aryl halides on the Pd⁰, which is responsible for the higher Heck reaction activity. Secondly, the reaction proceeds by coordination of alkene to the STOI, followed by its syn-migratory insertion. Subsequently, the newly generated organometallic species undergoes syn β-hydride elimination to form the Heck coupling product. Finally, base-assisted elimination of H-X from H-PdAu_r-X/Fe₃O₄@LDH species occurs to regenerate the Pd⁰ catalyst, and the intrinsic basic sites of the LDH phase may promote this elimination to some extent, as revealed in previous report [58].



Scheme 2. Plausible mechanism for the Heck reaction of aryl halides with alkenes over the $x\text{-PdAu}_r/\text{Fe}_3\text{O}_4@LDH$ catalysts.

3.6 Recyclability

The recyclability of the magnetic PdAu alloy NCs catalysts is further explored in the Heck reaction of PhI (1 mmol) and styrene (1.5 mmol) over $1.0\text{-PdAu}_{0.16}/\text{Fe}_3\text{O}_4@LDH$ (Pd: 0.3 mol%) and K_2CO_3 (3 mmol) in DMF- H_2O solvent. After completion of the reaction, the catalyst was magnetically separated from the reaction mixture by an NdFeB magnet (0.15 T), thoroughly washed with DMF and H_2O , and then reused under identical conditions and the results show 95% PhI Conv. and 90% trans-stilbene Sel. even in the 10th run (Fig. S10a). The SEM image of the recovered catalyst distinctly depicts the well-kept honeycomb-like core@shell structure (Fig. S10b). Moreover, only 3.5 wt% of total Pd and 3.3 wt% of total Au leached into the supernatant as confirmed by ICP (detection limit of 0.01 ppm) of the used catalyst after 10 runs. The $\text{Pd}^0/(\text{Pd}^{\text{II}} + \text{Pd}^0)$ ratio calculated from the Pd 3d XPS of the used catalyst (Fig. S10c) is 69.0%, significantly lower than that of the fresh one (93.1%), which can be ascribed to the high reactivity of PhI molecules that results in the high number of surface species, similar to Choudary's report on LDH-Pd⁰ [11]. The surface Au/Pd ratio of ~ 0.77 (Fig. S10c and d) is close to that of the fresh one (0.73), demonstrating that the surface metal composition of $\text{PdAu}_{0.16}$ alloy NCs was well-kept during the Heck reaction. These results clearly suggest the remarkable structure stability and recycling efficiency of the as-obtained magnetic PdAu alloy NCs catalysts.

4. Conclusions

In summary, a series of hierarchically core@shell structured magnetic PdAu alloy nanoclusters catalysts $x\text{-PdAu}_r/\text{Fe}_3\text{O}_4@LDH$ were facile assembled via polyol reduction followed sol immobilization of $\text{PdAu}_r\text{-PVP}$ on the honeycomb-like core@shell support $\text{Fe}_3\text{O}_4@LDH$. The characterization results reveal that the obtained catalysts possess the honeycomb-like core@shell structure with the *ab*-plane of hexagonal LDH nanoplates vertically oriented growth on the surface of Fe_3O_4 core, and the ultrafine PdAu alloy nanoclusters with the size ranging from 1.70 to 2.55 nm highly dispersed on the LDH nanoplates. The size and size distribution, electron density and surface composition of PdAu alloy NCs on the catalysts can be effectively tuned by Au-doping amount. Three catalysts $1.0\text{-PdAu}_r/\text{Fe}_3\text{O}_4@LDH$ (r : 0.11, 0.16 and 0.48) all present higher Heck reactivity of iodobenzene with styrene than the monometallic catalysts under the optimal condition of K_2CO_3 as base additive and DMF- H_2O ($v_{\text{DMF}}/v_{\text{H}_2\text{O}}=3:1$) as solvent,

attributable to the highly dispersed ultrafine PdAu NCs, increased surface Pd⁰ electron density and remarkable enhanced PdAu NCs – LDH – Fe_3O_4 three-phase synergistic effect. Particularly, $1.0\text{-PdAu}_{0.16}/\text{Fe}_3\text{O}_4@LDH$ with the smallest PdAu alloy NCs and the largest surface Pd⁰ electron density exhibits the highest Heck activity. Moreover, the obtained catalysts can be applied for Heck reaction of a variety of aryl halides with alkenes, and can be simply separated by an external permanent magnet and reused after ten runs without significant loss of activity, rendering its long-term stability. The present hierarchically core@shell structured magnetic PdAu alloy nanoclusters catalysts may open a new vision to develop novel environmentally benign magnetic bimetallic alloy catalysts for varied catalytic applications.

Acknowledgements

The work was supported by the National Natural Science Foundation of China (21576013).

Appendix A. Supplementary material

Supplementary data associated with this article can be found in the online version, at <http://dx.doi.org/>

References

- [1] T. Mizoroki, K. Mori, A. Ozaki, *Bull. Chem. Soc. Jap.* 44 (1971) 581.
- [2] R.F. Heck, J.P. Nolley, *J. Org. Chem.* 37 (1972) 2320–2322.
- [3] J. Choi, G.C. Fu, *Science* 356 (2017) 7230–7237.
- [4] B.M. Trost, J.D. Knopf, C.S. Brindle, *Chem. Rev.* 116 (2016) 15035–15088.
- [5] K. Rousée, J.P. Bouillon, S. Couve-Bonnaire, X. Pannecoucke, *Org. Lett.* 18 (2016) 540–543.
- [6] Á. Molnár, *Chem. Rev.* 111 (2011) 2251–2320.
- [7] M. Khajehzadeh, M. Moghadam, *J. Organomet. Chem.* 863 (2018) 60–69.
- [8] D. Liu, C. Zhang, F. Wang, Z.Y. Huang, N.S. Zhang, H.H. Zhou, Y.F. Kuang, *J. Mater. Chem. A* 3 (2015) 16583–16589.
- [9] M. Gholinejad, C. Najera, F. Hamed, M. Seyedhamzeh, M. Bahrami, M. Kompany-Zareh, *Tetrahedron* 73 (2017) 5585–5592.
- [10] A.K. Rathi, M.B. Gawande, J. Pechousek, J. Tucek, C. Aparicio, M. Petr, O. Tomanec, R. Krikavova, Z. Travnicek, R.S. Varma, R. Zboril, *Green Chem.* 18 (2016) 2363–2373.
- [11] B.M. Choudary, S. Madhi, N.S. Chowdari, M.L. Kantam, B. Sreedhar, *J. Am. Chem. Soc.* 124 (2002) 14127–14136.
- [12] Z. Feng, Q.Q. Min, H.Y. Zhao, J.W. Gu, X. Zhang, *Angew. Chem. Int. Edit.* 54 (2015) 1270–1274.
- [13] C. Chen, Q. Zheng, S.L. Ni, H.J. Wang, *New J. Chem.* 42 (2018) 4624–4630.
- [14] A. Bruneau, M. Roche, M. Alami, S. Messaoudi, *ACS Catal.* 5 (2015) 1386–1396.
- [15] A. Chakravarty, G. De, *Dalton Trans.* 45 (2016) 12496–12506.
- [16] N. Agarwal, S.J. Freakley, R.U. McVicker, S.M. Althabhan, N. Dimitratos, Q. He, D.J. Morgan, R.L. Jenkins, D.J. Willock, S.H. Taylor, C.J. Kiely, G.J. Hutchings, *Science* 358 (2017) 223–227.
- [17] J.H. Zhong, X. Jin, L.Y. Meng, X. Wang, H.S. Su, Z.L. Yang, C.T. Williams, B. Ren, *Nature Nanotech.* 12 (2016) 132–136.
- [18] R.N. Dhital, C. Kamonsatikul, E. Somsook, K. Bobuatong, M. Ehara, S. Karanjit, H. Sakurai, *J. Am. Chem. Soc.* 134 (2012) 20250–20253.
- [19] L.F. Tan, X.L. Wu, D. Chen, H.Y. Liu, X.W. Meng, F.Q. Tang, *J. Mater. Chem. A* 1 (2013) 10382–10388.

- [20] H.M. Song, B.A. Moosa, N.M. Khashab, *J. Mater. Chem. M* 22 (2012) 15953–15959.
- [21] L. Zhou, C. Gao, W. Xu, *J. Langmuir* 26 (2010) 11217–11225.
- [22] B. Karimi, F. Mansouri, H. Vali, *Green Chem.* 16 (2014) 2587–2596.
- [23] R. Ma, P.B. Yang, F.L. Bian, *New J. Chem.* 42 (2018) 4748–4756.
- [24] J.F. Yu, Q. Wang, D. O'Hare, L.Y. Sun, *Chem. Soc. Rev.* 46 (2017) 5950–5974.
- [25] F. Mi, X.T. Chen, Y.W. Ma, S.T. Yin, F.L. Yuan, H. Zhang, *Chem. Commun.* 47 (2011) 12804–12806.
- [26] S.T. Yin, J. Li, H. Zhang, *Green Chem.* 18 (2016) 5900–5914.
- [27] T. Fan, D.K. Pan, H. Zhang, *Ind. Eng. Chem. Res.* 50 (2011) 9009–9018.
- [28] L. Li, L.G. Dou, H. Zhang, *Nanoscale* 6 (2014) 3753–3763.
- [29] S. Nishimura, Y. Yakita, M. Katayama, K. Higashimine, K. Ebitani, *Catal. Sci. Technol.* 3 (2013) 351–359.
- [30] J.P. Ge, Y.X. Hu, M. Biasini, W.P. Beyermann, Y.D. Yin, *Angew. Chem. Int. Ed.* 46 (2007) 4342–4345.
- [31] P.S. Braterman, Z.P. Xu, F. Yarberry, In *Handbook of layered materials*; S. M. Auerbach, Eds. K. A. Carrado, P. K. Dutta, Marcel Dekker, New York, 2004, pp. 373.
- [32] K. Nakamoto, In *Handbook of Vibrational Spectroscopy*; J. M. Chalmers, Eds. P.R. Griffiths, John Wiley & Sons, New York, 2006, Vol. 3.
- [33] H. Chen, F. Zhang, S. Fu, X. Duan, *Adv. Mater.* 18 (2006) 3089–3093.
- [34] J.Y. Xian, Q. Hua, Z.Q. Jiang, Y.S. Ma, W.X. Huang, *Langmuir* 28 (2012) 6736–6741.
- [35] J.A. Gursky, S.D. Blough, C. Luna, C. Gomez, A. N. Luevano, E.A. Gardner, *J. Am. Chem. Soc.* 128 (2006) 8376–8377.
- [36] A.R. Denton, N.W. Ashcroft, Vegard's law, *Phys. Rev. A.* 43 (1991) 3161.
- [37] M. Tukhani, F. Panahi, A. Khalafi-Nezhad, *ACS Sustainable Chem. Eng.* 6 (2018) 1456–1467.
- [38] J.H. Yang, D.F. Wang, W.D. Liu, X. Zhang, F.L. Bian, W. Yu, *Green Chem.* 15 (2013) 3429–3437.
- [39] Y.M.A. Yamada, Y. Yuyama, T. Sato, S. Fujikawa, Y. Uozumi, *Angew. Chem. Int. Ed.* 53 (2014) 127–131.
- [40] M.E. Martínez-Klimov, P. Hernandez-Hipólito, T.E. Klimova, D.A. Solís-Casados, M. Martínez-García, *J. Catal.* 342 (2016) 138–150.
- [41] A. Zhou, R.M. Guo, J. Zhou, Y.B. Dou, Y. Chen, J.R. Li, *ACS Sustainable Chem. Eng.* 6 (2018) 2103–2111.
- [42] J.F. Moulder, W.F. Stickel, P.E. Sobol, K.D. Bomben, *Handbook of X-ray Photoelectron Spectroscopy*, J. Chastain, Perkin-Elmer, Minnesota, 1992.
- [43] Z.X. Li, W. Xue, B.T. Guan, F.B. Shi, Z.J. Shi, H. Jiang, C.H. Yan, *Nanoscale* 5 (2013) 1213–1220.
- [44] J. Xu, T. White, P. Li, C.H. He, J.G. Yu, W.K. Yuan, Y.F. Han, *J. Am. Chem. Soc.* 132 (2010) 10398–10406.
- [45] X. Yang, D. Chen, S. Liao, H. Song, Y. Li, Z. Fu, Y. Su, *J. Catal.* 291 (2012) 36–43.
- [46] J. Pritchard, L. Kesavan, M. Piccinini, Q. He, R. Tiruvalam, N. Dimitratos, J.A. Lopez-Sanchez, A.F. Carley, J.K. Edwards, C.J. Kiely, G.J. Hutchings, *Langmuir* 26 (2010) 16568–16577.
- [47] K. Qian, W. Huang, *Catal. Today* 164 (2011) 320–324.
- [48] L. Pauling, *The Nature of the Chemical Bond*, Cornell University Press, New York, 1960, pp. 93.
- [49] N.E. Kolli, L. Delannoy, C. Louis, *J. Catal.* 297 (2013) 79–92.
- [50] L.L. Zhang, A.Q. Wang, J.T. Miller, X.Y. Liu, X.F. Yang, W.T. Wang, L. Li, Y.Q. Huang, C.Y. Mou, T. Zhang, *ACS Catal.* 4 (2014) 1546–1553.
- [51] M.S. Chen, D. Kumar, C.W. Yi, D.W. Goodman, *Science* 310 (2005) 291.
- [52] Y.F. Pu, J.L. Zhang, X. Wang, H.Y. Zhang, L. Yu, Y.Z. Dong, W. Li, *Catal. Sci. Technol.* 4 (2014) 4426–4432.
- [53] F. Cárdenas-Lizana, S. Gómez-Quero, A. Hugon, L. Delannoy, C. Louis, *J. Catal.* 262 (2009) 235–243.
- [54] H. Zhang, G.Y. Zhang, X. Bi, X.T. Chen, *J. Mater. Chem. A* 1 (2013) 5934–5942.
- [55] L. Chmielarz, M. Jabłońska, A. Strumiński, Z. Piwowarska, A. Węgrzyn, S. Witkowski, M. Michalik, *Appl. Catal. B* 130–131 (2013) 152–162.
- [56] S. Song, H. Yang, R. Rao, H. Liu, A. Zhang, *Appl. Catal. A* 375 (2010) 265–271.
- [57] F.J. Berry, L.E. Smart, P.S.S. Prasad, N. Lingaiah, P.K. Rao, *Appl. Catal. A* 204 (2000) 191–201.
- [58] X.J. Jin, K. Taniguchi, K. Yamaguchi, N. Mizuno, *Chem. Sci.* 7 (2016) 5371–5383.

Facile synthesis of magnetic recyclable palladium-gold alloy nanoclusters catalysts PdAu_r/Fe₃O₄@LDH and its catalytic applications in Heck reaction

Jin Li[‡], Yajuan Wang[‡], Shunwang Jiang and Hui Zhang^{*}

Highlights

- Magnetic PdAu nanoclusters catalysts via facile polyol reduction-sol immobilization
- The ultrafine 1.0-PdAu_{0.16}/Fe₃O₄@LDH showing the highest Heck activity
- Electron-rich surface Pd⁰ species and the strongest PdAu NCs-LDH-Fe₃O₄ synergy
- Remarkable recycling efficiency upon magnetic separation